Orbital
The electronic journal of chemistry

the electronic journal of chemistry

Full Paper | http://dx.doi.org/10.17807/orbital.v16i4.21174

Leaf Extract Mediated Green Synthesis of Iron-oxide Nanoparticles (FeO -NPs) by Using *Hibiscus rosa-sinensis* (China rose): A Potential Approach and its Biological Application

Anjali Singh, Ruchi Bharti*, Ajay Thakur, Monika Verma, and Renu Sharma

The aim of this study was to synthesize iron oxide nanoparticles (NPs) using an aqueous extract obtained from the leaves of *Hibiscus rosa-sinensis*, commonly known as China rose. By employing an environmentally friendly approach, the production of small-sized and highly stable FeO-NPs was achieved, offering promising prospects for environmental preservation by eliminating the need for harmful chemicals. The synthesis process involved the extraction of the plant material through decoction, followed by the reaction with ferrous sulphate ($FeSO_4$) at room temperature for one hour. Various analytical techniques, including Fourier transform infrared spectroscopy (FTIR), UV-visible spectrophotometry (UV-Vis), X-ray diffraction (XRD), and scanning electron microscopy-energy dispersive X-ray analysis (SEM-EDX), were employed to characterize the synthesized FeO-NPs. Additionally, their antioxidant activity was evaluated against 2,2-azino-bis-3-ethylbenzothiazoline-6-sulphonic acid (ABTS) and 2,2-diphenyl-1-picrylhydrazyl (DPPH). The results indicated that FeO-NPs derived from *Hibiscus rosa-sinensis* possessed significant antioxidant properties, suggesting their potential utility in various applications.

Graphical abstract

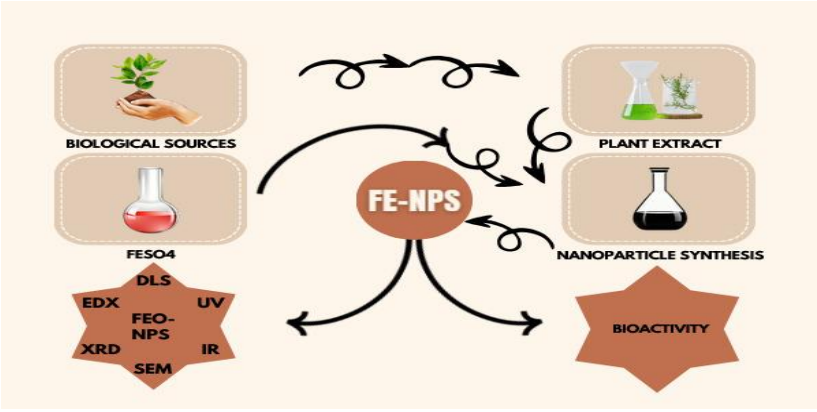

Keywords

Antioxidant activity
FeO-NPs
Hibiscus rosa-sinensis
Green synthesis
Characterization

Article history

Received 19 May 2024
Revised 08 Oct 2024
Accepted 08 Nov 2024
Available online 08 Jan 2025

Handling Editor: Ana C. Micheletti

1. Introduction

Nanoparticles (NPs) represent a diverse class of materials characterized by their size, typically less than 100 nm [1]. These materials exhibit a wide range of properties that find application across various sectors, including medical, pharmaceutical, manufacturing, environmental, electronics, energy collection, and mechanical industries. Nanomaterials

Department of Chemistry, Institute of Sciences, Chandigarh University, Mohali, Punjab, 140413, India. *Corresponding author. E-mail: ruchi.uis@cumail.in

can take various forms, including carbon nanotubes, fullerenes, metallic, ceramic, nanorods, nano capsules, nano emulsions, and polymer NPs [2]. In recent years, there has been a growing interest in metallic NPs due to their unique properties and potential applications in catalysis, composite materials, disease diagnosis and treatment, and sensor technologies [3-5]. Among the various metal nanoparticles, iron nanoparticles (IONPs) offer prospective advantages in numerous domains.

Iron oxide, occurring naturally in different phases and widely distributed, has been extensively studied due to its variable oxidation states, crystal structures, low cost, magnetic properties, and environmental acceptability [6-10]. Iron oxide nanoparticles have found applications in biomedical fields, environmental remediation, food analysis, immunoassays, magnetic targeted drug delivery, lithium-ion batteries, photoelectrochemical cells, and catalysis [11-13].

The synthesis of metal nanoparticles can be achieved through various techniques, including chemical, physical, and green synthesis methods. Chemical synthesis often involves the use of chemical agents, resulting in significant chemical waste and environmental contamination [14]. Physical techniques, such as gamma irradiation, pulse laser ablation, and spark discharge, are efficient but require expensive equipment [15]. In recent decades, there has been a surge in plant-mediated green synthesis of nanoparticles, leveraging plant extracts as biogenic agents [1]. This approach offers several advantages, including affordability, simplicity, atom economy, benignity, nontoxicity, removal of hazardous elements, and ease of availability [16-18]. Utilizing plant extracts for nanoparticle synthesis has emerged as an environmentally friendly and cost-effective alternative to traditional methods, aiming to mitigate the negative impacts associated with chemically generated nanoparticles [19].

In this study, we aim to synthesize iron oxide nanoparticles (IONPs) using the plant extract of *Hibiscus rosa-sinensis*. *Hibiscus rosa-sinens*is, also known as "china rose" or "japakusum," is a significant medicinal plant belonging to the family Malvaceae. Found in tropical and subtropical regions, including India, *Hibiscus rosa-sinensis* has demonstrated anti-inflammatory, antimicrobial, antioxidant, and antipyretic properties, particularly in its flowers and leaves [20-21]. Phytochemical analysis has revealed the presence of various bioactive compounds in *Hibiscus rosa-sinensis*, including tannins, flavonoids, phenols, alkaloids, terpenoids, saponins, and essential oils [22]. Quantitative analysis has further highlighted the abundance of flavonoids, phenolics, tannins, carbohydrates, proteins, vitamins, and minerals in *Hibiscus rosa-sinensis* flowers, highlighting its potential as a biogenic agent for nanoparticle synthesis [22].

In this study, we introduce an eco-friendly method for synthesizing IONPs utilizing the plant extract of *Hibiscus rosa-sinensis*. The process involves characterizing these nanoparticles through various techniques, followed by an evaluation of their antioxidant potential.

2. Material and Methods

Chemicals

Ferrous sulfate heptahydrate ($FeSO_4.7H_2O$), a pivotal precursor essential for the synthesis of iron oxide nanoparticles, was procured from Sigma Aldrich, a globally recognized supplier renowned for its premium-grade chemical reagents. The high-quality standards upheld by Sigma Aldrich ensured the reliability and consistency crucial for the successful execution of experimental procedures. In addition to Ferrous sulfate heptahydrate, other essential chemicals utilized in the antioxidant assays were also sourced from Sigma Aldrich. These included 2,2-azino-bis-3-ethylbenzothiazoline-6-sulphonic acid (ABTS), a common reagent employed in assessing antioxidant activity, and 2,2-diphenyl-1-picrylhydrazyl (DPPH), another widely used compound for evaluating radical scavenging properties. Furthermore, Gallic Acid and Ascorbic Acid, standard reference antioxidants utilized for comparison in the antioxidant assays, were also acquired from Sigma Aldrich. Their procurement from the same reputable supplier ensured uniformity and consistency in the experimental procedures, eliminating the need for further purification and guaranteeing the reliability of the obtained results.

Collection of Plant Material

Fresh leaves of *Hibiscus rosa-sinensis* were diligently harvested from the lush herbal garden of Chandigarh University during their peak growth phase, ensuring the maximum retention of phytochemical constituents vital for nanoparticle synthesis. The freshly plucked leaves underwent thorough cleaning by successive rinsing with deionized water to remove any adhering impurities or contaminants. Subsequently, the cleaned leaves were carefully air-dried for approximately one hour under ambient conditions in a shaded environment to preserve their inherent properties. Once dried, the leaves were gently fragmented into smaller pieces to facilitate extraction of their bioactive components.

Preparation of *Hibiscus rosa- sinensis* Plant Extract

To prepare the plant extract, 30 g of the dried *Hibiscus rosa-sinensis* leaves were precisely weighed and then immersed in 200 mL of deionized water within a beaker. The aqueous mixture was then subjected to controlled heating, maintaining a temperature range between 70 to 80 degrees Celsius, for a duration of one hour to facilitate efficient extraction of bioactive compounds from the plant material. Following the extraction process, the resultant solution was allowed to cool to room temperature and subsequently filtered using high-quality Whatman filter paper to remove any solid debris or insoluble particles. The filtration process ensured the separation of the *Hibiscus rosa-sinensis* leaf extract from any residual plant material, yielding a clear and homogeneous solution ready for further experimentation.

Synthesis Procedure of Iron oxide nanoparticles

Ferrous sulfate heptahydrate ($FeSO_4{\cdot}7H_2O$) served as the precursor for synthesizing FeO nanoparticles in this study. Initially, 2.78 g of $FeSO_4{\cdot}7H_2O$ were precisely dissolved in distilled water to prepare a 0.1 M $FeSO_4$ solution with a volume of 100 mL. The synthesis process involved combining 50 mL of the prepared $FeSO_4$ solution with an equal volume of *Hibiscus rosa-sinensis* leaf extract, establishing a 1:1 volume ratio. Subsequently, 50 mL of this freshly prepared $FeSO_4$ solution were carefully added dropwise to 50 mL of the plant extract with constant stirring over a period of five hours at room temperature. Throughout this time, the solution's color transitioned from a pale-yellow hue to a deep black, indicative of the reduction of iron ions and the formation of FeO nanoparticles. Upon completion of the reaction, the resulting solution underwent centrifugation for 30 minutes to separate the solid nanoparticles from the liquid phase. Following centrifugation, the supernatant was discarded, and the solid

residue was washed multiple times with ethanol to remove any residual impurities. Finally, the washed FeO nanoparticles were collected and allowed to dry for 18 hours at 30 degrees Celsius in an oven. The dried FeO nanoparticles were then subjected to various characterization techniques to assess their structural, morphological, and chemical properties.

Characterization of FeO NPs

Various characterization techniques were employed to comprehensively analyze the synthesized FeO nanoparticles. Fourier Transform Infrared (FT-IR) analysis, conducted using a Perkin Elmer Spectrum 2 instrument, examined the nanoparticles' functional groups within the spectral range of 400 cm^{-1} to 4000 cm^{-1}, providing insights into their chemical composition and structure. Scanning Electron Microscopy (SEM) with energy-dispersive X-ray (EDX) was carried out using a JSM IT 500 instrument analysis facilitated high-resolution imaging and elemental composition determination, respectively, elucidating the morphology and elemental content of the nanoparticles. X-ray diffraction (XRD) analysis, was carried using a Bruker D8 Advance instrument performed with Cu-Kα radiation, unveiled the crystalline structure, phases, and crystal orientation of the Fe nanoparticles. Dynamic Light Scattering (DLS) studies, conducted using the Zetasizer Advance instrument, offered valuable insights into the size distribution profile and stability of the nanoparticles in solution, enhancing understanding of their colloidal behavior. Together, these characterization techniques provided a comprehensive understanding of the structural, morphological, chemical, and colloidal properties of the synthesized FeO nanoparticles.

Antioxidant Activity

DPPH (2,2-diphenyl-1-picrylhydrazyl) activity of iron nanoparticles

The DPPH (2,2-diphenyl-1-picrylhydrazyl) assay is a widely used method for evaluating antioxidant activity based on hydrogen transfer. This assay employs a synthetic, stable radical, DPPH, which undergoes reduction in the presence of antioxidants. The protocol for the DPPH assay involved preparing a DPPH solution by dissolving 4 mg of DPPH in 100 mL of methanol. Subsequently, 3mL of the DPPH solution was mixed with 200 µL of the sample solution, prepared in methanol at a concentration of 1 mg per mL. The mixture was thoroughly mixed and incubated in the dark for 30 minutes to allow for the reaction to occur. The absorbance of the DPPH solution was measured using a UV-visible spectrophotometer at 517 nm [23-25], both before and after adding the nanoparticle (NP) solutions. The antioxidant activity was determined by calculating the percentage of DPPH scavenged using

% DPPH Scavenging = [(A control - A sample) / A control] × 100,

where A control represents the absorbance of the DPPH solution without the sample, and A sample represents the absorbance of the DPPH solution with the sample added.

ABTS [2,2'-azino-bis (3-ethylbenzothiazoline-6-sulphonic acid)] assay

Various assays utilize the ABTS radical cation method to assess the antioxidant activity of compounds or materials. In this study, the ABTS assay was employed to evaluate the antioxidant capacity of the synthesized nanoparticles. Initially, the absorbance of the ABTS solution was measured at 734 nm using a UV-visible spectrophotometer [23-25]. This initial absorbance reading provides a baseline measure of the ABTS radical cation's absorbance. Subsequently, the nanoparticle (NP) solution was added to the ABTS solution, and the absorbance was measured again at the same wavelength after a specified incubation period. The decrease in absorbance indicates the scavenging ability of the nanoparticles towards the ABTS radical cation, reflecting their antioxidant activity. The percentage of ABTS scavenging was calculated using

% ABTS Scavenging = (A - B / A) × 100,

where A represents the initial absorbance of the ABTS solution, and B represents the absorbance of the ABTS solution after the addition of the nanoparticle solution. This quantitative approach provides valuable insights into the antioxidant potential of the synthesized nanoparticles, allowing for comparisons with known antioxidants and further characterization of their biological properties.

3. Results and Discussion

In the pursuit of expanding the biomedical applications of nanoparticles (NPs), it becomes imperative to devise synthesis methods that are both non-toxic and environmentally sustainable. Therefore, the primary objective of this research was to develop a synthetic approach utilizing *Hibiscus rosa-sinensis* leaf extract for the production of FeO-NPs. In this process, solutions containing ferrous sulphate heptahydrate ($FeSO_4.7H_2O$) and *Hibiscus rosa-sinensis* leaf extract were allowed to stand at ambient temperature. Remarkably, the color of the solution swiftly transitioned from yellow to black, indicating the formation of Fe-NPs within the extract (Fig. 1). The incorporation of the leaf extract into the ferrous sulphate heptahydrate solution served as the source of iron precursor, facilitating the synthesis of FeO-NPs.

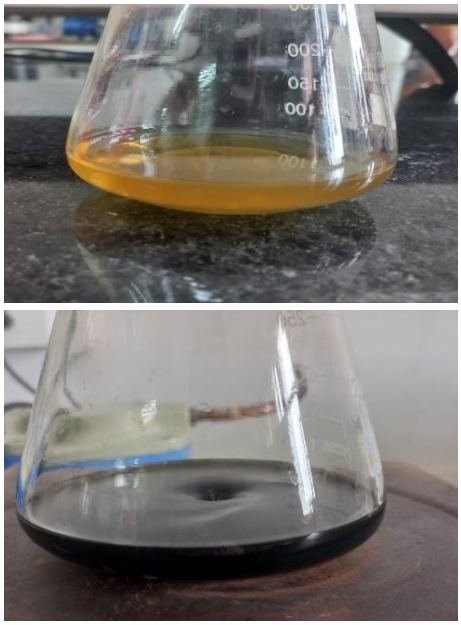

Fig. 1. Color change of the reaction mixture from yellow to black.

Fourier Transform Infrared Spectroscopy

Infrared spectroscopy, a powerful analytical tool, allows for the identification of functional groups within molecules

based on their characteristic absorption bands in the infrared region. In this study, Fourier-transform infrared (FTIR) spectroscopy was employed to analyze the chemical composition of both the plant extract and the synthesized FeO nanoparticles (NPs). The FTIR spectra obtained for the plant extract, depicted in Figure 2 (a), revealed distinctive absorption peaks, each indicative of specific functional groups presents in the extract. Notably, the prominent peak observed at 3334.33 cm-1 corresponded to the stretching vibrations of the O-H group, indicative of the presence of hydroxyl functional groups. Additionally, peaks observed at 1636.93 cm-1and 415.59 cm^{-1} were attributed to the stretching vibrations of the C=O group, suggesting the presence of carbonyl functionalities and alkyl halide within the extract. Upon the introduction of $FeSO_4$ and subsequent synthesis of FeO nanoparticles, significant alterations in the FTIR spectra were observed, as illustrated in Figure 2 (b). The synthesized FeO nanoparticles exhibited a distinct set of IR peaks at 3335 cm^{-1}, 1626 cm^{-1}, 1387 cm^{-1}, 1244 cm^{-1}, 1071 cm^{-1}, and 537 cm^{-1}. These new peaks indicated changes in the chemical composition and structure compared to the plant extract alone. The absorption band observed at 3335 cm^{-1} suggests the presence of O-H stretching vibrations, similar to those observed in the plant extract, indicating the retention of hydroxyl groups on the surface of the FeO nanoparticles. The peak at 1626 cm^{-1} may correspond to the stretching vibrations of the C=O group, indicating the presence of carbonyl functionalities, possibly from organic compounds adsorbed onto the nanoparticle surface or inherent in the FeO structure. Additionally, peaks observed at 1387 cm^{-1}, 1244 cm^{-1}, 1071 cm^{-1}, and 537 cm^{-1} may arise from various molecular vibrations associated with the FeO nanoparticles, providing further insights into their chemical composition and structural characteristics. Overall, the FTIR analysis facilitated the elucidation of functional groups present in both the plant extract and the synthesized FeO nanoparticles, offering valuable information about their chemical nature and potential interactions.

SEM analysis with EDX of FeO NPs

The comprehensive characterization of the Fe nanoparticles (Fe-NPs) encompassed a detailed examination of their structure, surface morphology, and elemental composition using advanced analytical techniques such as scanning electron microscopy (SEM) imaging and energy-dispersive X-ray spectroscopy (EDX). The SEM images provided valuable insights into the physical appearance of the FeO-NPs, revealing their cuboidal shape with noticeable irregularities observed in localized regions, suggesting variations in particle size or aggregation patterns (Fig. 3).

Furthermore, the elemental composition of the synthesized FeO-NPs was elucidated through EDX analysis (Fig. 3, Table 1), a technique capable of quantifying the relative abundance of different elements present in the sample. The EDX spectrum obtained from the FeO-NPs confirmed the presence of key elements, with predominant peaks corresponding to iron (Fe) and oxygen (O). Interestingly, a notable proportion of sulfur (S) was also detected in the EDX spectrum, indicating its contribution to the elemental composition of the nanoparticles. It is noteworthy that the sulfur signal observed in the EDX spectrum is attributed to the residual presence of sulfur from the precursor materials used during the synthesis process, such as ferrous sulfate heptahydrate ($FeSO_4.7H_2O$). Despite the careful purification steps employed during synthesis, trace amounts of sulfur may persist in the final product, as evidenced by the EDX analysis. This residual sulfur content, although minimal, highlights the importance of thorough characterization and quality control measures in nanoparticle synthesis protocols.

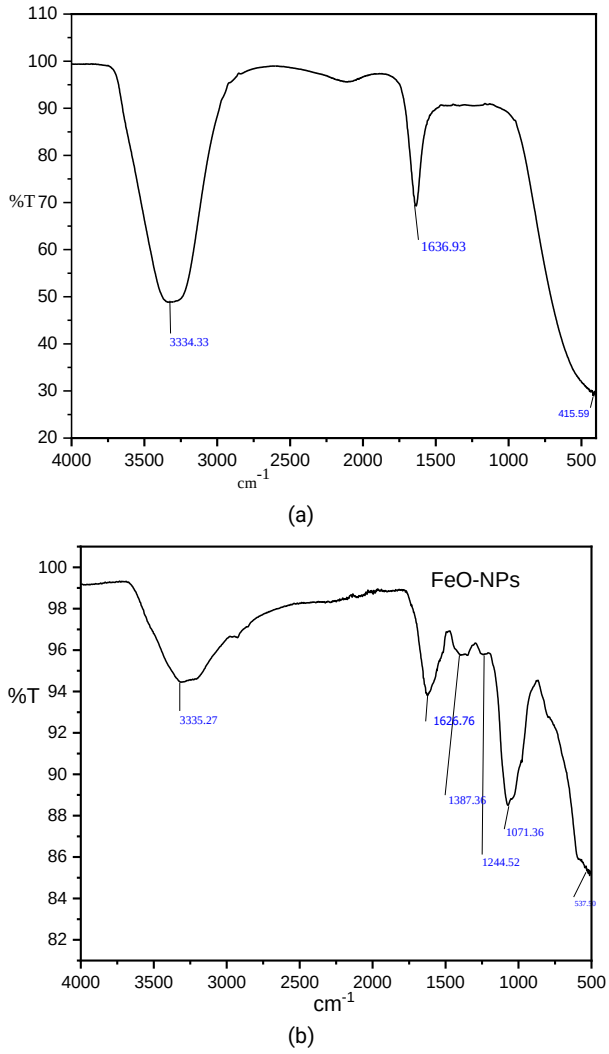

Fig. 2. FTIR spectra of (a) plant extract (b) iron oxide NPs.

Table 1. SEM EDX analysis of the synthesized iron oxide nanoparticles.

Element	Line	Mass%	Atom%
Fe	K	48.12 ± 1.98	22.97± 0.94
O	K	40.62± 0.90	67.68± 1.51
S	K	11.26± 0.47	9.36± 0.39
Total		100.00	100.00

Dynamic light scattering (DLS)

The results of the analysis reveal that the Z-average size of the nanoparticles, a measure of the mean hydrodynamic diameter, is determined to be 382.2 nm (Fig. 4). This parameter indicates the average size of the particles in the sample, with a higher value suggesting larger particle sizes. In our case, the Z-average value of 382.2 nm indicates that the nanoparticles exhibit a substantial size, which is typically within the nano-scale range, making them suitable for various applications.

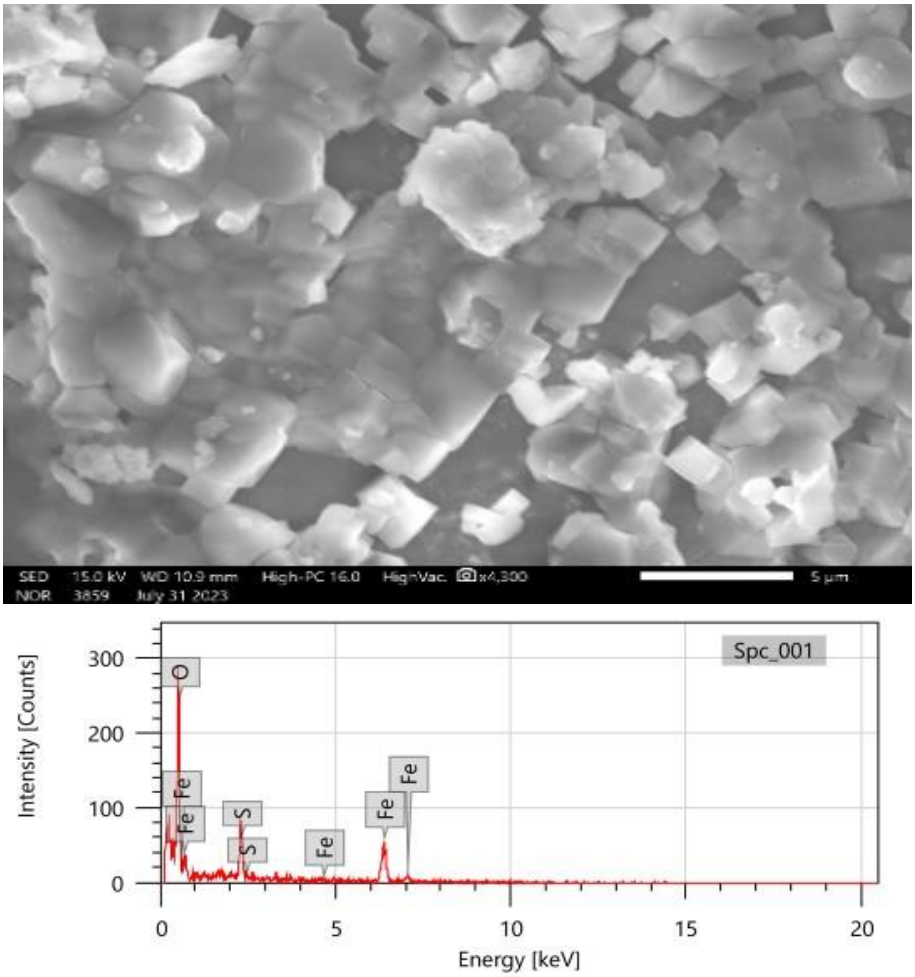

Fig. 3. SEM analysis with EDX of FeO NPs.

The Polydispersity Index (PI) is a measure of the uniformity of particle size distribution within a sample. A PI value of 1 indicates a monodisperse sample, meaning that all particles have nearly identical sizes. In our analysis, the PI value of 1 suggests a homogeneous size distribution among the nanoparticles, indicating that they are relatively uniform in size. The intercept value of 1.092 and fit error of 0.006133 are parameters associated with the fitting of the data during the analysis process. These values reflect the accuracy and reliability of the measurement method used to determine the particle size distribution. A lower fit error indicates a better fit of the data to the model, enhancing the confidence in the obtained results. The "In Range" percentage of 76.49% indicates the proportion of nanoparticles that fall within the specified size range. In our analysis, this value suggests that a significant majority of the nanoparticles meet the size criteria, making them suitable for the intended application. However, it is essential to consider the specific requirements of the application and ensure that the nanoparticles meet the desired size specifications. Furthermore, the mean peak intensity, ordered by area, is determined to be 335.2 nm. This parameter provides additional insight into the size distribution of the nanoparticles, with a higher intensity indicating a greater abundance of particles of a particular size. In our case, the mean peak intensity suggests that a considerable proportion of nanoparticles exhibit sizes around 335.2 nm.

In summary, the comprehensive analysis of the nanoparticle size distribution reveals that the nanoparticles exhibit uniform size distribution, with a predominant population falling within the desired size range. These findings are crucial for understanding the physical characteristics of the nanoparticles and evaluating their suitability for various applications, including biomedical, environmental, and technological applications.

X-ray Diffraction Analysis

X-ray powder diffraction (XRD) analysis stands as a pivotal technique in elucidating the structural properties and phase composition of materials, including nanoparticles. In this study, XRD was instrumental in characterizing the synthesized FeO nanoparticles (NPs), providing valuable insights into their crystalline structure. The XRD pattern of the FeO NPs, illustrated in Fig. 5, was meticulously obtained over a range of 2θ angles spanning from 10 to 100 degrees at room temperature. As noted by Yadav et al. [26], the observed XRD pattern unveiled the amorphous nature of the FeO NPs synthesized in this study. This revelation was evident through the characteristic broadening of diffraction peaks, particularly notable at lower intensities. Unlike their nanocrystalline counterparts, which typically exhibit well-defined Bragg peaks, the amorphous form of iron oxide nanoparticles is distinguished by the absence of such peaks and the presence of broadened diffraction profiles. Indeed, the XRD pattern showcased a distinctive broad hump indicative of amorphous FeO NPs, extending from 2θ = 25° to 2θ = 37°, with a pronounced peak centered at 2θ = 29.16°. This broadening and lack of sharp peaks underscored the absence of long-range crystalline order in the synthesized FeO NPs, reaffirming their amorphous structural nature.

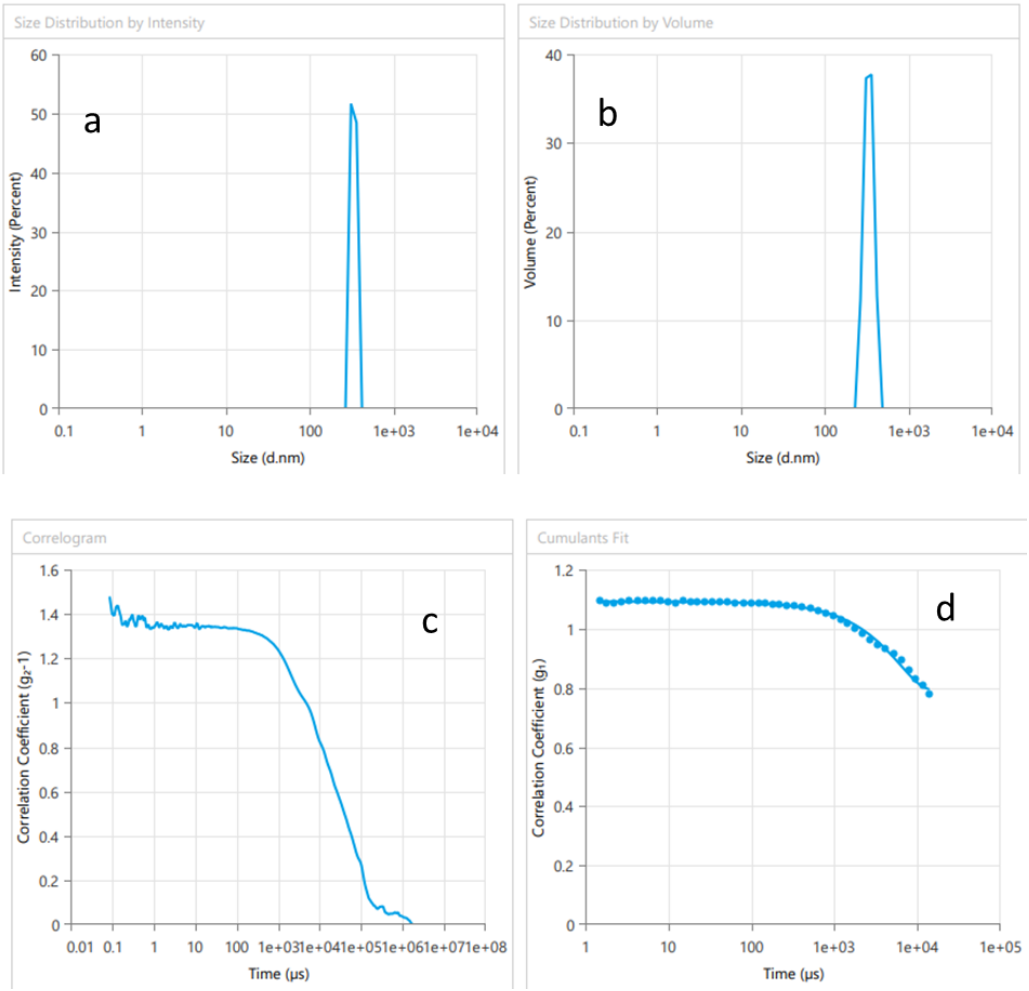

Fig. 4. Size distribution (a, b), Correlogram (c) and Comulants fit diagram obtained by DLS data.

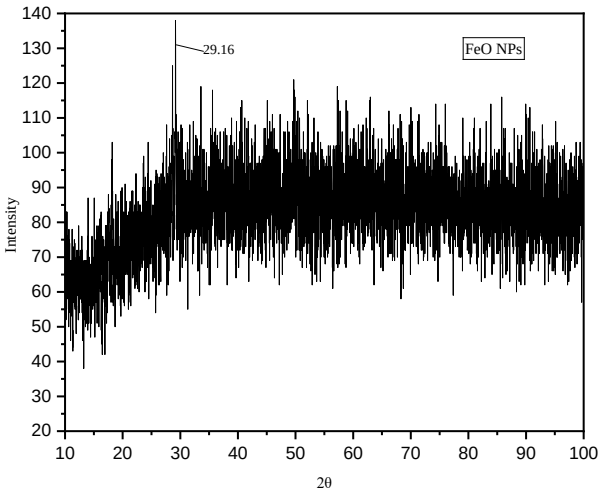

Fig. 5. XRD pattern of iron oxide nanoparticles.

Anti-oxidant assay

The antioxidant activity of the synthesized nanoparticles was assessed using two widely employed assays: the DPPH (2,2-diphenyl-1-picrylhydrazyl) and ABTS (2,2'-azino-bis(3-ethylbenzothiazoline-6-sulfonic acid)) assays. Gallic Acid and Ascorbic Acid were included as reference standards for comparative analysis. In the DPPH assay, the nanoparticles demonstrated a substantial scavenging activity, with an inhibition percentage of 97.05%. In contrast, in the ABTS assay, the scavenging activity was relatively lower, with an inhibition percentage of 42.91%. Gallic Acid exhibited robust antioxidant potential, displaying % inhibition values of 91.76% ± 0.62 and 96.53% ± 0.15 in the DPPH and ABTS assays, respectively. Similarly, Ascorbic Acid showed significant antioxidant activity, with % inhibition values of 96.53% ± 0.15 and 97.65% ± 0.15 in the DPPH and ABTS assays, respectively. These findings highlight the notable antioxidant efficacy of the synthesized nanoparticles, suggesting their potential utility in various biomedical and industrial applications requiring antioxidant properties. Additionally, a comparison of antioxidant activity with literature data is presented in Table 2, further emphasizing the efficacy of IONPs in these roles.

Table 2. Comparison of antioxidant activity of the synthesized compounds with the literature.

Sr. No.	Plant Used	ABTS	DPPH	Ref.
1.	*Hibiscus rosa-sinensis*	42.91%	97.05%	Present Work
2.	*Bacillus circulans*	39.44%	35.44%	[27]
3.	*Coriandrumsativum L.*	-	32.54% to 84.28%	[28]
4.	*Plumeria obtusa*	-	70.23%	[29]
5.	*Rhamnus virgata*	-	79.4%	[30]

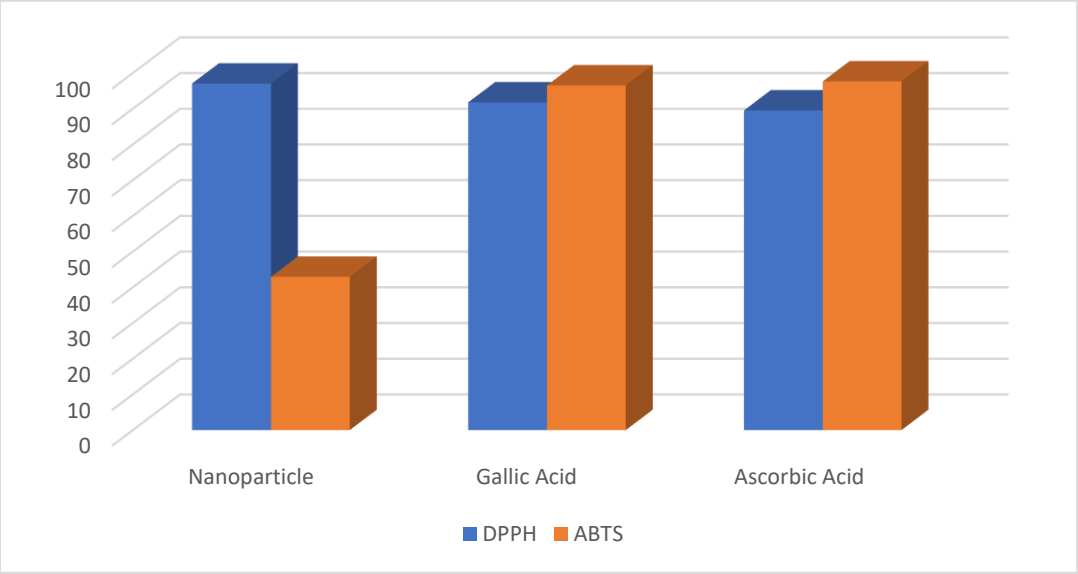

Fig. 7. Antioxidant Activity Comparison.

4. Conclusions

In conclusion, our study showcases the potential of employing eco-friendly methodologies for the synthesis of nanoparticles (NPs), particularly focusing on the production of FeO-NPs using *Hibiscus rosa sinensis* leaf extract. Through a series of comprehensive characterizations including Fourier transform infrared spectroscopy (FTIR), scanning electron microscopy (SEM), X-ray diffraction (XRD), energy dispersive X-ray (EDX) analysis, and antioxidant activity assays, we have successfully confirmed the synthesis and properties of FeO-NPs. Our findings highlight the effectiveness of the green synthesis approach, offering a non-toxic, environmentally benign, and straightforward alternative to conventional NP synthesis methods. The crystallinity, elemental composition, morphology, and functional groups of the synthesized FeO-NPs were elucidated, providing valuable insights into their structural and chemical properties. Additionally, the demonstrated antioxidant activity showcased the potential biomedical and environmental applications of these NPs. Overall, our study contributes to the growing body of research on sustainable NP synthesis methods and highlights the promising role of plant-mediated approaches in addressing the demand for eco-friendly nanomaterial production.

Acknowledgments

The authors express their sincere appreciation to Chandigarh University for generously providing the essential laboratory facilities that were crucial for conducting this research. Additionally, the authors would like to convey their appreciation to Punjab University and Chandigarh University for granting access for the analytical facilities, which greatly contributed to the successful execution of this research study.

Author Contributions

Anjali Singh performed the experiments, calculations, analyzed the data and wrote the manuscript. Ruchi Bharti and Ajay Thakur helped in the analysis of results and writeup. They have been also involved to design the research and literature survey. Monika Verma helped in interpretation of various spectra and formatting. Ruchi Bharti and Renu Sharma did the final review of the manuscript.

References and Notes

[1] Thakur, A.; Verma, M.; Bharti, R.; Sharma, R. *Curr. Chin. Sci.* **2023**, *3*, 322. [Crossref]

[2] Pourmadadi, M.; Eshaghi, M. M.; Ostovar, S.; Mohammadi, Z.; Sharma, R. K.; Paiva-Santos, A. C.; Pandey, S. *J. Drug Delivery Sci. Technol.* **2023**, *82*, 104357. [Crossref]

[3] Mukherjee, S.; Patra, C. R. *Future Sci. OA* **2017**, *3*, 203. [Crossref]

[4] Darabdhara, G.; Das, M. R.; Singh, S. P.; Rengan, A. K.; Szunerits, S.; Boukherroub, R. *Adv. Colloid Interface Sci.* **2019**, *271*, 101991. [Crossref]

[5] John, A.; Benny, L.; Cherian, A. R.; Narahari, S. Y.; Varghese, A.; Hegde, G. *J. Nanostruct. Chem.* **2021**, *11*, 1. [Crossref]

[6] Roszczenko, P.; Szewczyk, O. K.; Czarnomysy, R.; Bielawski, K.; Bielawska, A. *Pharmaceutics* **2022**, *14*, 2286. [Crossref]

[7] Khandel, P.; Yadaw, R. K.; Soni, D. K.; Kanwar, L.; Shahi, S. K. *J. Nanostruct. Chem.* **2018**, *8*, 217. [Crossref]

[8] Liu, S.; Regulacio, M. D.; Tee, S. Y.; Khin, Y. W.; Teng, C. P.; Koh, L. D.; Guan, G.; Han, M. Y. *The Chemical Record* **2016**, *16*, 1965. [Crossref]

[9] Waychunas, G. A.; Kim, C. S.; Banfield, J. F. *J. Nanopart. Res.* **2005**, *7*, 409. [Crossref]

[10] Ahmad, W.; Kumar Jaiswal, K.; Amjad, M. *Inorg. Nano-Met. Chem.* **2021**, *51*, 1147. [Crossref]

[11] Etemadi, H.; Buchanan, J. K.; Kandile, N. G.; Plieger, P. G. *ACS Biomater. Sci. Eng.* **2021**, *7*, 5432. [Crossref]

[12] Low, L. E.; Lim, H. P.; Ong, Y. S.; Siva, S. P.; Sia, C. S.; Goh, B. H.; Chan, E. S.; Tey, B. T. *J. Controlled Release 2022*, *345*, 231. [Crossref]

[13] Devi, H. S.; Boda, M. A., Shah, M. A.; Parveen, S.; Wani, A. H. *Green Process. Synth.* **2019**, *8*, 38. [Crossref]

[14] Mahdavi, M.; Namvar, F.; Ahmad, M. B.; Mohamad, R. *Molecules* **2013**, *18*, 5954. [Crossref]

[15] Ramesh, P. S.; Kokila, T.; Geetha, D. *Spectrochim.* **2015**, *142*, 339. [Crossref]

[16] Abdullah, J. A. A.; Eddine, L. S.; Abderrhmane, B.; Alonso-González, M.; Guerrero, A.; Romero, A. *Sustainable Chem. Pharm.* **2020**, *17*, 100280. [Crossref]

[17] Saravanakumar, A.; Peng, M. M.; Ganesh, M.; Jayaprakash, J.; Mohankumar, M.; Jang, H. T. *Artif. Cells, Nanomed., Biotechnol.* **2017**, *45*, 1165. [Crossref]

[18] Naseem, T.; Farrukh, M. A. *J. Chem.* **2015**, *2015*, 912342. [Crossref]

[19] Buarki, F.; AbuHassan, H.; Al Hannan, F.; Henari, F. Z. *J. Nanotechnol.* **2022**, *2022*, 5474645. [Crossref]

[20] Magdalita, P. M.; San Pascual, A. O. *Floriculture and Ornamental Plants* **2020**, *2020*, 1. [Crossref]

[21] Kombaiah, K.; Vijaya, J. J.; Kennedy, L. J.; Bououdina, M. *Ceram. Int.* **2016**, *42*, 2741. [Crossref]

[22] Suprabha, D.; Avilash, R.; Paul, A.; Saha, N.; Tarafdar, A.; Mazumder, S. *Sustainability, Agri, Food and Environmental Research* **2023**, *12*, 1. [Crossref]

[23] Thakur, A.; Bharti, R.; Verma, M.; Sharma, R.; Sharma, A.; Gupta, A.; Sharma, V. *Synthesis* **2023**, *55*, 3129. [Crossref]

[24] Verma, M.; Thakur, A.; Kapil, S.; Sharma, R.; Sharma, A.; Bharti, R. *Mol. Diversity* **2023**, *27*, 889. [Crossref]

[25] Thakur, A.; Verma, M.; Setia, P.; Bharti, R.; Sharma, R.; Sharma, A.; Bansal, R. *Res. Chem. Intermed.* **2023**, *49*, 859. [Crossref]

[26] Yadav, V. K.; Yadav, K. K.; Gnanamoorthy, G.; Choudhary, N.; Khan, S. H.; Gupta, N.; Kamyab, H.; Bach, Q. V. *Environ. Technol. Innovation* **2020**, *20*, 101089. [Crossref]

[27] Rabani, G.; Dilshad, M.; Sohail, A.; Salman, A.; Ibrahim, S.; Zafar, I.; Arshad, H. M. *J. Chem.* **2023**, *2023*, 4659034. [Crossref]

[28] Singh, K.; Chopra, D. S.; Singh, D.; Singh, N. *Arabian J. Chem.* **2020**, *13*, 9034. [Crossref]

[29] Perveen, S.; Nadeem, R.; ur Rehman, S.; Afzal, N.; Anjum, S.; Noreen, S.; Saeed, R.; Amami, M.; Al-Mijalli, S. H.; Iqbal, M. *Arabian J. Chem.* **2022**, *15*, 103764. [Crossref]

[30] Abbasi, B. A.; Iqbal, J.; Mahmood, T.; Qyyum, A.; Kanwal, S. *Appl. Organomet. Chem.* **2019**, *33*, 4947. [Crossref]

How to cite this article

Singh, A.; Bharti, R.; Thakur, A.; Verma, M.; Sharma, R. *Orbital: Electron. J. Chem.* **2024**, *16*, 271. http://dx.doi.org/10.17807/orbital.v16i4.21174